^6Li and ^7Li NMR in the $LiNi_{1-y}Co_yO_2$ Solid Solution ($0 \leq y \leq 1$)

Claire Marichal, Jérôme Hirschinger,* and Pierre Granger

Institut de Chimie, UMR 50 CNRS, Bruker Spectrospin, Université Louis Pasteur, BP 296/R8, 67008 Strasbourg Cedex, France

Michel Ménétrier, Aline Rougier, and Claude Delmas

Laboratoire de Chimie du Solide du CNRS and Ecole Nationale Supérieure de Chimie et Physique de Bordeaux, Université de Bordeaux I, 351 cours de la Libération, 33405 Talence Cedex, France

Received May 27, 1994[⊗]

A series of phases belonging to the $LiNi_{1-y}Co_yO_2$ ($0 \leq y \leq 1$) solid solution have been studied by ^6Li and ^7Li NMR. Static and magic-angle-spinning (MAS) spin-echo NMR experiments have been carried out at two magnetic field strengths (4.7 and 7.1 T). The ^6Li and ^7Li high-speed MAS spectra are found to be sensitive to hyperfine couplings with both the nearest and next nearest nickel neighbors. These short distance interactions are used to yield information on the distribution of the transition metal atoms in the (Ni, Co)O_2 slabs. While deviations from a random Ni/Co distribution cannot be quantified by NMR experiments on static samples, the MAS spectra clearly demonstrate that the $LiNi_{1-y}Co_yO_2$ phases have a tendency to form cobalt clusters. These results show that, in favorable circumstances, MAS NMR of paramagnetic materials permits the accurate detection of short scale heterogeneities that cannot be observed by X-ray diffraction.

Introduction

In recent years, the $LiNiO_2$ and $LiCoO_2$ oxides have been the subject of a great deal of scientific and technological interest in relation to their use as positive electrode materials for secondary lithium batteries.[1−4] In particular, the use of the solid solution $LiNi_{1-y}Co_yO_2$ between these two systems appears to be a promising way to optimize the electrochemical properties of this type of material.[5−7] Although X-ray diffraction clearly shows that these phases exhibit the classical layered structure generally found for most AMO_2 oxides, with the presence of some additional Ni^{2+} ($t_2^6e^2$) ions in the interlayer (lithium) sites for $y \leq 0.3$,[5,8] this technique gives no information on the distribution of the Co^{3+} (LS t_2^6) and Ni^{3+} (LS $t_2^6e^1$) ions within the $Ni_{1-y}Co_yO_2$ slabs. However, such information is necessary for any detailed understanding of the electronic structure and, possibly, the electrochemical properties of these materials.

During the last decade, "high-resolution solid-state NMR" spectroscopy has become a standard technique for studying molecular order and dynamics.[9,10] Indeed, in a strong magnetic field B_0, most of the line broadenings due to chemical shift anisotropy and dipole−dipole and quadrupolar interactions can often be suppressed by high-speed magic-angle-spinning (MAS).[11−13] However, although NMR in paramagnetic materials originated in the middle 1950's with the study of bonding in transition metal fluoride single crystals,[14,15] only a few applications of the MAS technique to paramagnetic powders have appeared.[16−20] These results nevertheless demonstrate that, under appropriate conditions, the paramagnetic ions provide a means for the determination of structural information.[19,20] In particular, ^6Li and ^7Li MAS NMR was recently shown to be very useful for studying the local environment of the lithium atoms inserted in vanadium oxide bronzes that are also used as cathode material in secondary batteries.[21]

In this work, we use ^6Li and ^7Li static and high-speed MAS NMR in order to characterize the structure of the $LiNi_{1-y}Co_yO_2$ phases ($0 \leq y \leq 1$). As suggested by a preliminary ^7Li NMR study,[22] the spectra which are sensitive to short distance couplings with the Ni^{3+} ions may be related to the Ni/Co distribution.

Experimental Section

A. Sample Preparation. The $LiNi_{1-y}Co_yO_2$ ($0 \leq y \leq 1$) phases have been prepared by direct reaction from Li_2CO_3, NiO, and Co_3O_4 in stoichiometric proportions. The finely ground mixtures have been heated to 500 °C for a few hours and then for 48 h under O_2 in the 800−1000 °C temperature range (depending on the cobalt content). The materials made were found to be homogeneous in the whole composition range by X-ray powder diffraction.[5,23]

B. NMR Measurements. ^6Li ($I = 1$) and ^7Li ($I = 3/2$) NMR measurements were carried out at room temperature on Bruker MSL-

* Corresponding author.

[⊗] Abstract published in *Advance ACS Abstracts,* March 1, 1995.

(1) Thomas, M. G. S. R.; David, W. I. F.; Goodenough, J. B. *Mater. Res. Bull.* **1985**, *20*, 1137.
(2) Mizushima, K.; Jones, P. C.; Wiseman, P. J.; Goodenough, J. B. *Mater. Res. Bull.* **1980**, *15*, 783.
(3) Delmas, C.; Braconnier, J. J.; Hagenmuller, P. *Mater. Res. Bull.* **1982**, *17*, 117.
(4) Mendiboure, A.; Delmas, C.; Hagenmuller, P. *Mater. Res. Bull.* **1984**, *19*, 1383.
(5) Delmas, C.; Saadoune, I. *Solid State Ionics* **1992**, *53*−56, 370.
(6) Delmas, C.; Saadoune, I.; Rougier, A. *J. Power Sources* **1993**, *43*−44, 595.
(7) Ohzuku, T.; Ueda, A.; Nagayama, M.; Iwakoshi, Y.; Komori, H. *Electrochim. Acta* **1993**, *38*, 1159.
(8) Zhecheva, E.; Stoyanova, R. *Solid State Ionics* **1993**, *66*, 143.
(9) Mehring, M. *Principles of High Resolution NMR in Solids*, 2nd ed.; Springer: Berlin, 1983.
(10) Fyfe, C. A. *Solid State NMR for Chemists*; CFC Press: Guelph, Ontario, Canada, 1983.
(11) Andrew, E. R.; Bradbury, A.; Eades, R. G. *Nature* **1958**, *182*, 1659.
(12) Lowe, I. J. *Phys. Rev. Lett.* **1959**, *2*, 285.
(13) Maricq, M. M.; Waugh, J. S. *J. Chem. Phys.* **1979**, *70*, 3300.
(14) Bleaney, B. *Phys. Rev.* **1956**, *104*, 1190.
(15) Shulman, R. G.; Jaccarino, V. *Phys. Rev.* **1957**, *108*, 1219.
(16) Rothwell, W. P.; Waugh, J. S.; Yesinowski, J. P. *J. Am. Chem. Soc.* **1980**, *102*, 2637.
(17) Oldfield, E.; Kinsey, R. A.; Smith, K. A.; Nichols, J. A.; Kirkpatrick, R. J. *J. Magn. Reson.* **1983**, *51*, 325.
(18) Cheetham, A. K.; Dobson, C. M.; Grey, C. P.; Jakeman, R. J. B. *Nature* **1987**, *328*, 706.
(19) Nayeem, A.; Yesinowski, J. P. *J. Chem. Phys.* **1988**, *89*, 4600.
(20) Brough, A. R.; Grey, C. P.; Dobson, C. M. *J. Am. Chem. Soc.* **1993**, *115*, 7318.
(21) Hirschinger, J.; Mongrelet, T.; Marichal, C.; Granger, P.; Savariault, J. M.; Déramond, E.; Galy, J. *J. Phys. Chem.* **1993**, *97*, 10301.
(22) Ménétrier, M.; Rougier, A.; Delmas, C. *Solid State Commun.* **1994**, *90*, 439.

0020-1669/95/1334-1773$09.00/0

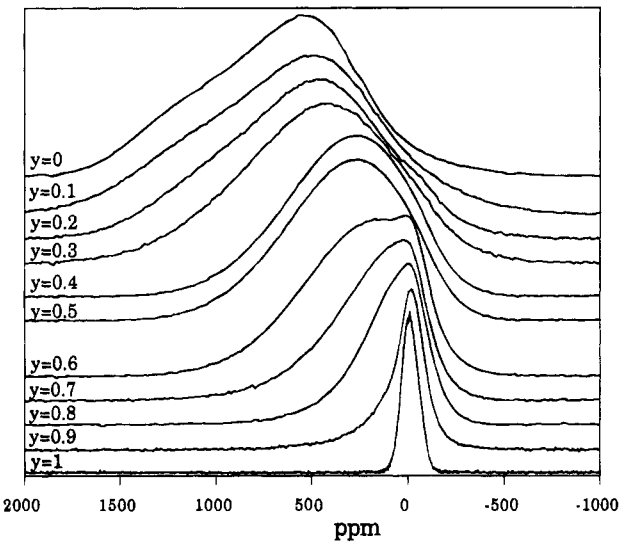

Figure 1. ^{7}Li static spin-echo line shapes for the series of $LiNi_{1-y}Co_yO_2$ ($0 \leq y \leq 1$) solid solution samples at $B_0 = 7.1$ T.

300 ($B_0 = 7.1$ T, Larmor frequency $\nu_0 = 44.150$ and 116.598 MHz in ^{6}Li and ^{7}Li resonance, respectively) and ASX-200 ($B_0 = 4.7$ T, $\nu_0 = 77.751$ MHz in ^{7}Li resonance) spectrometers. For experiments on static samples, a standard broad-band Bruker probe was used. MAS spectra were obtained by using a Bruker high-speed MAS probe with cylindrical 4-mm-o.d. zirconia rotors. Spinning frequencies ν_r up to 15 kHz were utilized. Due to the presence of a large paramagnetic shift interaction, the free induction decay (fid) following a single radio-frequency pulse is very rapid (a few microseconds) for both static and, to a lesser extent, rotating samples (see below). A significant part of the signal is then lost during the receiver dead time ($\approx 4-10$ μs). This results in severe distortions of the NMR spectrum.[24,25] Therefore, the dead time problem has been overcome by applying the well-known two-pulse spin-echo sequence[24,26]

$$\theta_1-\tau_1-\theta_2-\tau_2-\text{acquire}-D_0$$

where θ_1 and θ_2 are the radio frequency (RF) pulse angles and τ_1, τ_2 are delay times. τ_1 ranged from 70 to 100 μs, and a recycle time D_0 of 1 to 2 s was found to be long enough to avoid T_1 saturation effects. In the MAS experiments, the spin echo was synchronized with the first rotational echo in order to obtain a complete refocusing of the magnetization;[19,27] i.e., τ_1 was fixed to the rotor period $T_r = 1/\nu_r \approx 70-90$ μs. Moreover, although we observed that T_2 relaxation results in some intensity losses at the echo, especially for high nickel contents in ^{7}Li resonance ($T_2 \approx 500$ μs when $y = 0.5$), identical spectra were obtained as τ_1 was increased from T_r to $2T_r$ and $3T_r$. Hence, for these short τ_1 delays, no significant T_2 echo distortions are detected (all the spectral lines have decreased by essentially the same amount), so that the MAS synchronized spin-echo technique effectively gives a quantifiable signal. Spectral widths between 50 kHz and 1.667 MHz were used. After left shifting, the spin-echo signal is Fourier transformed with no line broadening starting at the top of the echo ($\tau_2 < \tau_1$) to yield an undistorted NMR spectrum. The isotropic shifts, reported in parts per million, are relative to an external sample of 1.0 M LiCl solution in H_2O.

All Lorentzian peak fittings of the NMR spectra were performed on a Silicon Graphics 4D/25 computer running Felix 2.1 NMR software.

Results and Discussion

A. Static Sample. Figure 1 shows the experimental spectra in ^{7}Li resonance resulting from the application of a spin-echo sequence of two 1-μs RF pulses ($\theta_1 = \theta_2 \approx 25°$) to the series of $LiNi_{1-y}Co_yO_2$ solid solution samples ($0 \leq y \leq 1$). The short pulse length prevents any significant finite pulse length distortions.[24] Moreover, only the sign (not the amplitude) of the spin echo appears to be changed by the relative phase of the two RF pulses (in-phase or quadrature). This fact is the first evidence for the presence of a strong shift anisotropy.[21,28] Thus, the 16-step phase cycling proposed by Rance and Byrd[24] causing destructive interference of the fid tails but coaddition of the spin-echo signals was employed. For $LiCoO_2$ ($y = 1$), a featureless line shape of *ca.* 12 kHz width and centered at the resonance of LiCl (0 ppm) is obtained. Note that the ^{7}Li spin-echo spectra of both $LiCoO_2$ and $LiNiO_2$ are in good agreement with previous reported data.[29,30] On the other hand, as previously observed in one-pulse experiments,[22] the NMR spectra of the solid solution samples may be decomposed into (at least) two components. Indeed, the introduction of nickel atoms can be associated with the apparition of a broader line shape component which is strongly positively shifted and whose fraction progressively increases with the concentration of nickel (Figure 1). This latter signal may be attributed to lithium ions interacting with at least one nickel atom as first 3d neighbors (component I) while the narrower signal at 0 ppm (component II) which stays similar to the $LiCoO_2$ spectrum would correspond to lithium sites with only cobalt in their first coordination sphere.[22] For $y < 0.50$, component I seems to be representative of almost the entire NMR signal; i.e., there must then be a very small fraction of Li^+ ions with only cobalt as their first 3d neighbors. However, components I and II are not resolved and both the width and isotropic shift of component I obviously depend on y (Figure 1). Hence, a deconvolution of the static spin-echo line shapes into these two components is precluded.

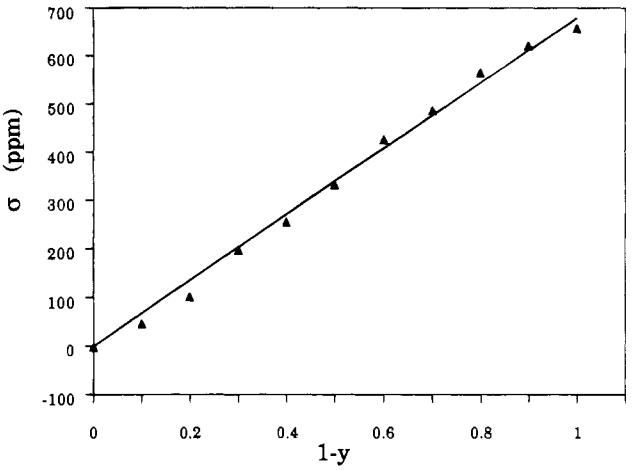

Figure 2. Variation of the isotropic shift of the spin-echo spectra (Figure 1) as a function of the nickel content. The solid line represents a least-squares fit of the data by eq 1.

Alternatively, we can easily extract the center of gravity or isotropic shift σ of the spectrum. Figure 2 shows that the experimental data are well fitted by a linear increase of σ as a function of the nickel content

$$\sigma(y) = C(1 - y) \qquad (1)$$

with a slope C of 679 ± 9 ppm.

The isotropic shift due to the coupling between an electronic and a nuclear moment or "hyperfine shift" can be expressed as

(23) Rougier, A.; Saadoune, I.; Gravereau, P.; Delmas, C. *Solid State Ionics* **1995**, in press.
(24) Rance, M.; Byrd, R. A. *J. Magn. Reson.* **1983**, *52*, 221.
(25) Heuer, A.; Haeberlen, U. *J. Magn. Reson.* **1989**, *85*, 79.
(26) Hahn, E. L. *Phys. Rev.* **1950**, *80*, 580.
(27) Olejniczak, E. T.; Vega, S.; Griffin, R. G. *J. Chem. Phys.* **1984**, *81*, 4804.
(28) Bonera, G.; Galimberti, M. *Solid State Commun.* **1966**, *4*, 589.
(29) Itoh, M.; Yamada, I.; Ubukoshi, K.; Hirakawa, K.; Yasuoka, H. *J. Phys. Soc. Jpn.* **1986**, *55*, 2125.
(30) Ganguly, P.; Ramaswamy, V.; Mulla, I. S.; Shinde, R. F.; Bakara, P. P.; Ganapathy, S.; Rajamohanan, P. R.; Prakash, N. V. K. *Phys. Rev. B* **1992**, *46*, 11595.

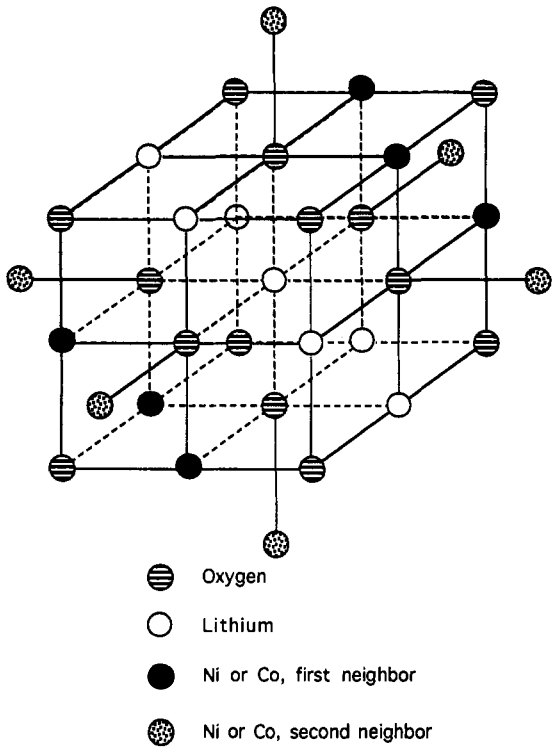

Figure 3. Idealized crystal structure of the $LiNi_{1-y}Co_yO_2$ solid solution. The first and second transition metal neighbors with respect to the central lithium ion are distinguished.

a sum of two terms:[31] (i) the (Fermi) contact shift arising from the unpaired electron density in the nucleus s orbital induced by interaction through the bonding electrons; (ii) the so-called pseudocontact shift corresponding to the trace of the electron–nuclear dipolar interaction which is nonvanishing when the electronic **g** tensor is anisotropic.[32]

In the $LiNi_{1-y}Co_yO_2$ solid solution, it may then be assumed that σ is predominantly due to the hyperfine shift $p\sigma_{hf}$ from the p nearest Ni^{3+} neighbors ($p = 0-6$)[29] belonging to two groups of three transition metal sites, facing each other in two adjacent layers, as shown in Figure 3. Since the NMR line intensity is proportional to the number of resonant spins in each environment, it also is proportional to the probability $P(y,p)$ for a given Li^+ ion to have p nearest Ni^{3+} neighbors. In the case of a random Ni/Co distribution, the isotropic shift is then written

$$\sigma(y) = \sum_{p=0}^{6} p\sigma_{hf}P(y,p) = \sigma_{hf}\sum_{p=0}^{6} p\binom{6}{p}(1-y)^p y^{6-p} \qquad (2)$$

where

$$\binom{n}{p}$$

is the binomial coefficient. Using the well-known relation

$$p\binom{n}{p} = n\binom{n-1}{p-1} \qquad (3)$$

eq 2 simply becomes

$$\sigma(y) = 6\sigma_{hf}(1-y) \qquad (4)$$

Equations 1 and 4 then lead to a value of 113 ± 2 ppm for σ_{hf}. Thus, it may be inferred from this simple model that the increase of σ due to the replacement of the diamagnetic Co^{3+} by the paramagnetic Ni^{3+} ions is well accounted for by a random

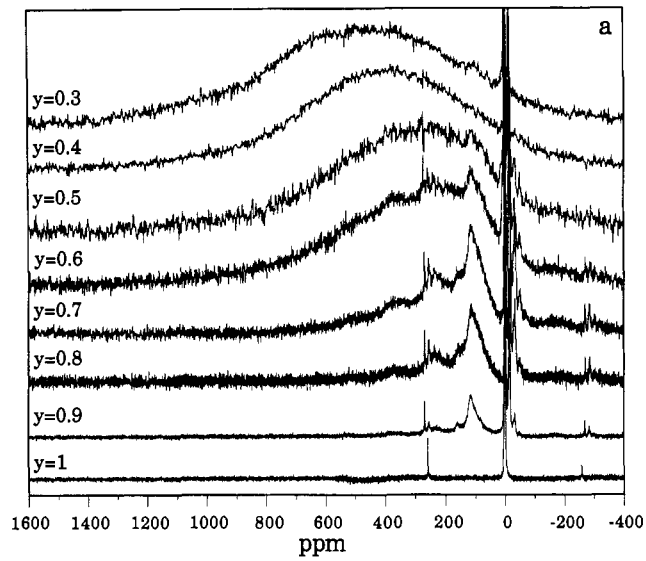

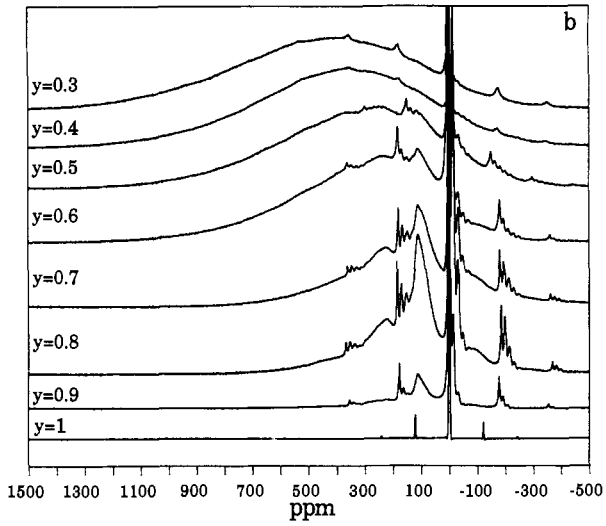

Figure 4. High-speed MAS spectra of the $LiNi_{1-y}Co_yO_2$ ($0.3 \leq y \leq 1$) solid solution phases: (a) ^6Li resonance for $B_0 = 7.1$ T; (b) ^7Li resonance for $B_0 = 4.7$ T.

distribution of the transition metal atoms within the (Ni, Co)O_2 slabs. However, the fact that component II is still observed in single pulse spectra for cobalt contents as small as $y = 0.3$ supports the existence of some cobalt segregation.[22] This may be reflected in the slight sigmoidal character of the increase of σ with increasing nickel content (Figure 2). Moreover, note that this analysis is not only limited to interaction with the nearest Ni^{3+} neighbors but also neglects possible Ni–O–Ni ferromagnetic couplings[29,30,33] as well as the presence of any interlayer Ni^{2+} ions.[5,8] Hence, it is concluded that more information is needed in order to quantify possible deviations from a random Ni/Co distribution.

B. Magic Angle Sample Spinning. Further information about the heterogeneous character of the NMR spectrum is provided by high-speed MAS NMR. Indeed, under MAS in a strong magnetic field, the anisotropic part of any nuclear spin interaction (e.g., shift, dipolar interaction, or quadrupolar interaction) is averaged to first order as long as the spinning frequency ν_r exceeds the width of the powder spectrum.[13] Moreover, in the case of an inhomogeneous interaction (e.g., shift or quadrupolar), the MAS spectrum is split into sharp spinning side bands separated by ν_r around the central line at the isotropic shift. Since the anisotropy information is then

(31) *NMR of Paramagnetic Molecules*; LaMar, G. N., Ed.; Academic Press: New York, 1973.
(32) McConnell, H. M.; Robertson, R. E. *J. Chem. Phys.* **1958**, *29*, 1361.
(33) Goodenough, J. B. *Magnetism and the Chemical Bond*; Wiley: New York, 1963.

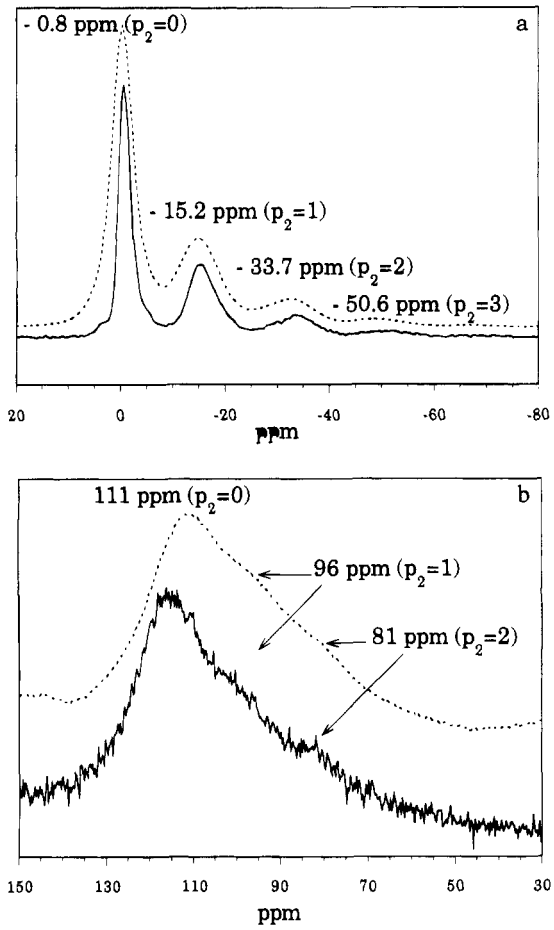

Figure 5. Hyperfine shifts in ^{6}Li (solid line) and ^{7}Li (broken line) resonances due to the interaction of the lithium nucleus with p_1 and p_2 Ni^{3+} ions in the first and the second coordination sphere, respectively: (a) $y = 0.7$, $p_1 = 0$; (b) $y = 0.9$, $p_1 = 1$.

contained in the side band intensities,[19,34] MAS allows separation of resonances in spectra with overlapping powder patterns.

Figure 4 shows the high speed ($\nu_r \approx 12-15$ kHz) MAS synchronized spin-echo spectra for the series of $LiNi_{1-y}Co_yO_2$ phases ($0.3 \leq y \leq 1$) in ^{6}Li and ^{7}Li resonances. Attempts to spin samples for $y < 0.3$ were unsuccessful, probably as a consequence of the presence of an excessively high macroscopic magnetization in these paramagnetic materials. Indeed, these compounds contain interlayer Ni^{2+} ions that may induce a magnetic coupling between the layers, in addition to the ferromagnetic couplings of the Ni^{3+} ions within one layer.[29,30,33] The 90°-pulse lengths being as short as 2.3 and 1.5 μs in ^{6}Li and ^{7}Li resonances, respectively, the pulse angles were set to their usual values, $(\theta_1, \theta_2) = (90°, 180°)$. Moreover, we checked that identical results are obtained with $\theta_1 = \theta_2 = 90°$. Figures 4 and 5 show that both ^{6}Li and ^{7}Li high-speed MAS NMR not only permits resolving the two main line shape components overlapping in static samples but also allows the observation of a fine structure within each component. Note that the use of a lower B_0 field in ^{7}Li resonance (4.7 T) permits one to place any rotational side bands of component II outside the region of overlap with the 50−140 ppm spectral range of interest (Figures 4b and 5b). Furthermore, we have observed that the center of gravity of the spectrum is similar to the one obtained in the static samples. This clearly confirms that the entire NMR signal is detected in both experiments. However, the spin-echo sequence must be used as in the case of a static sample in order to prevent any distortion and underestimation of the relatively broad component I, especially for low cobalt contents. Indeed, one-pulse MAS experiments show that component I is severely affected by the receiver dead time so that it cannot be easily resolved from the baseline distortions.[22,25] The increase of both the isotropic shift and line width of this latter signal with increasing nickel concentration is confirmed by the MAS experiments (Figure 4). On the other hand, with the introduction of Ni^{3+} ions, it can be seen that component II is split into a series of negatively shifted sharp peaks at *ca.* −15, −30, −45 ppm, etc. (Figure 5a) besides the peak at ≈0 ppm corresponding to the single type of lithium site existing in $LiCoO_2$. Note that ^{6}Li NMR offers a higher resolution while a better sensitivity is obtained in ^{7}Li resonance, as previously noticed in lithium-inserted vanadium oxide bronzes.[21] Moreover, the first spinning side bands at $\pm\nu_r$ and $\pm 2\nu_r$ from the isotropic peaks of component II which are also well detected, especially in ^{7}Li resonance (Figure 4b), show that the anisotropy of these resonances increases with the absolute value of the isotropic shift, as expected for dipole interactions of the lithium nuclear moment with an increasing number of paramagnetic nickel ions.[15,19,20] Although much less apparent, a fine structure is also observed in component I for high cobalt content ($y \geq 0.7$). Indeed, close inspection shows that a series of equidistant peaks, ≈15 ppm apart from each other, may be distinguished within the asymmetric peak whose maximum is in the range 110−115 ppm (Figure 5b). Furthermore, note that this shift value σ_{hf}^{I} is in excellent agreement with the hyperfine shift constant $\sigma_{hf} = 113$ ppm determined in the previous section. Hence, the high spectral resolution offered by high-speed MAS NMR demonstrates the presence of a small negative hyperfine shift constant $\sigma_{hf}^{II} \approx -15$ ppm in addition to the positive shift constant σ_{hf}^{I} which is large enough to be detectable in static samples. These two different shift constants of opposite sign may be attributed to the interaction of the Li nucleus with Ni^{3+} ions in the first two coordination spheres, each of these containing six transition metal atoms. Indeed, Figure 3 shows that the p orbitals of the oxygen atoms provide efficient pathways for electron transfer from both the nearest and next nearest nickel neighbors (contact shift). The large shift constant σ_{hf}^{I} is logically attributed to coupling with the first Ni^{3+} neighbors, 2.9 Å away from the lithium ion, as spin density may then be transferred directly to the lithium nucleus in addition to 90° Ni−O−Li indirect exchange involving orthogonal oxygen p orbitals.[15,35] On the other hand, since direct overlap of the lithium and nickel orbitals is impossible in the case of second nearest neighbors lying 4.1 Å away from the lithium ion (Figure 3), the anion must be playing the role of an intermediary (180° Ni−O−Li interaction), so that $|\sigma_{hf}^{II}|$ is expected to be smaller than $|\sigma_{hf}^{I}|$. Note that the p character of the bonds is also relevant to the superexchange process which ascribes long-range order to the magnetic properties of the intervening anions.[36] In this respect, it is remarked that the opposite signs of the hyperfine shifts attributed to 90° and 180° Ni−O−Li indirect couplings agree with the Goodenough−Anderson superexchange rules.[33,36] Figure 6 summarizes the interpretation of the high-speed MAS spectra.

Owing to the high resolution offered by the MAS technique, it may now be possible to extract site probabilities directly from the peak intensities, at least for component II. If the transition metal atoms are statistically distributed, the probability for a given Li^+ ion to have respectively p_1 and p_2 Ni^{3+} neighbors in the first and second coordination spheres (Figure 3) is written

$$P(y,p_1,p_2) = P(y,p_1)P(y,p_2) \qquad (5)$$

where $P(y,p)$ is defined in eq 2.

(34) Herzfeld, J.; Berger, A. E. *J. Chem. Phys.* **1980**, *73*, 6021.

(35) Shulman, R. G.; Sugano, S. *Phys. Rev.* **1963**, *130*, 506.

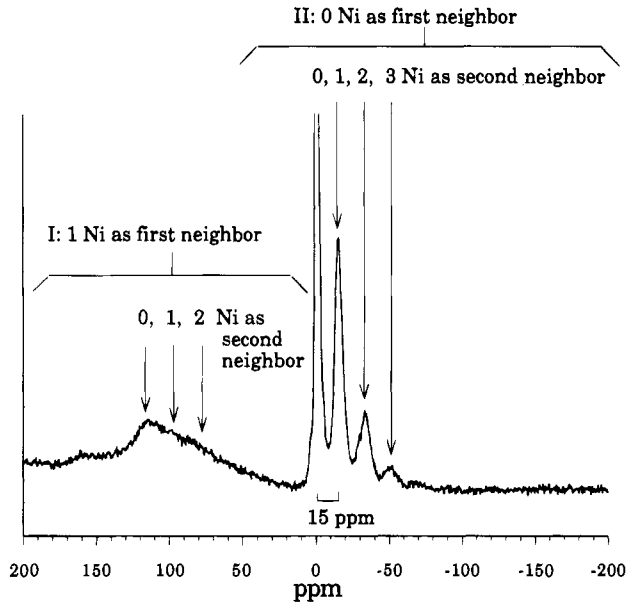

Figure 6. Assignment of the isotropic peaks observed in the high-speed MAS spectra.

The intensities $I(y,0,p_2)$ of the peaks shifted at *ca.* $p_2\sigma_{hf}^{II}$, i.e., corresponding to Li^+ ions with only cobalt as their first cationic neighbors ($p_1 = 0$) and with p_2 nickel atoms as their second cationic neighbors, are easily determined by Lorentzian peak fitting in both ^6Li and ^7Li resonances. The variation of $I(y,0,p_2)$ as a function of y is shown in Figure 7 for $p_2 = 0$, 1, 2, and 3, the remaining peaks ($p_2 > 3$) representing less than 1% of the total NMR signal. A good agreement between the ^6Li and ^7Li data is observed. Since T_2 relaxation times are longer in ^6Li resonance than in ^7Li resonance, this fact further confirms the quantitative reliability of our data. In Figure 7 are also reported the corresponding theoretical probabilities $P(y,0,p_2)$ and $P(y,p_1)$ with $p_1 = p_2$. First, it is seen that $I(y,0,p_2)$ strongly departs from $P(y,p_1)$ for $p_1 = p_2 > 0$. On the other hand, the discrepancies between $I(y,0,p_2)$ and $P(y,0,p_2)$ are of the same order for all the considered p_2 values. This further confirms that the first two coordination spheres must be included in the data analysis (the good agreement between $I(y,0,0)$ and $P(y,0)$ is fortuitous). Moreover, it is obvious from Figure 7 that $I(y,0,p_2)$ would be better described by $P(y',0,p_2)$ where y' is chosen to be somewhat higher than y, except for the low values of $I(y,0,2)$ and $I(y,0,3)$ when $y \leq 0.7$ (an explanation for this is provided below). In other words, the probability of having cobalt atoms (first sphere) surrounded by other cobalt atoms (second sphere) is significantly higher than predicted by a random Ni/Co distribution; i.e., there is formation of *cobalt clusters*. Hence, our results clearly show that the $LiNi_{1-y}Co_yO_2$ solid solution has a tendency to segregate, as already suggested by one-pulse experiments in static samples.[22]

Since component I is poorly resolved (Figure 4), it was not possible to extract all the site populations corresponding to lithium ions having more than one nickel atom as first 3d neighbors ($p_1 > 1$). The fraction $I(y,1)$ of the overlapping peaks

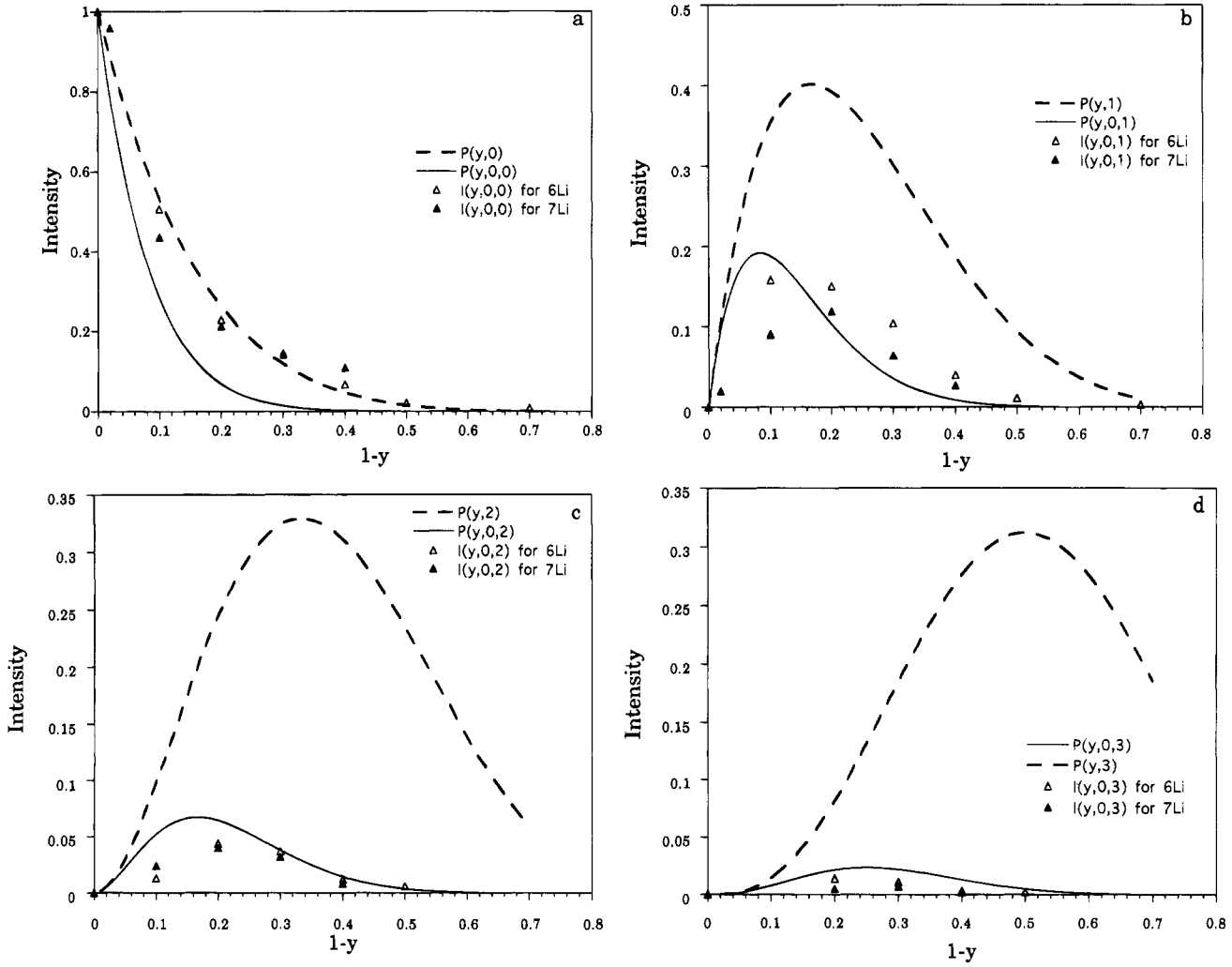

Figure 7. Comparison of the experimental peak intensities $I(y,0,p_2)$ in ^6Li (△) and ^7Li (▲) resonances with the theoretical probabilities $P(y,0,p_2)$ (solid line) and $P(y,p_1)$ with $p_1 = p_2$ (broken line) as a function of the nickel content: (a) $p_2 = 0$; (b) $p_2 = 1$; (c) $p_2 = 2$; (d) $p_2 = 3$.

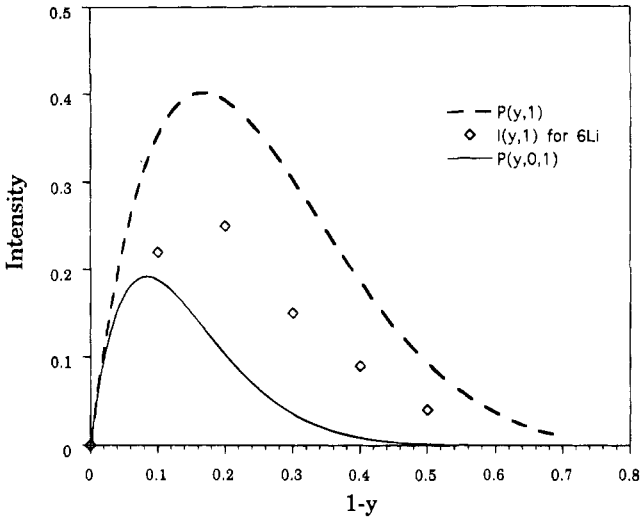

Figure 8. Comparison of the experimental peak intensities $I(y,1)$ in ^{6}Li resonance (◇) with the theoretical probabilities $P(y,0,1)$ (solid line) and $P(y,1)$ (broken line) as a function of the nickel content.

in the range 60−115 ppm corresponding to the case $p_1 = 1$ could nevertheless be selected by peak fitting in ^{6}Li resonance for $y \geq 0.5$ (Figures 4 and 5). Figure 8 shows that the experimental data lie between $P(y,1)$ and $P(y,0,1)$. For $y \geq 0.8$, these results are well accounted for by some segregation of the transition metal ions, as in the case of the $I(y,0,p_2)$ intensities (cf. above). On the other hand, the decrease of the peak intensities for highest nickel contents ($y \leq 0.7$) may be explained by an enhancement of the magnetic moments due to 90° Ni−O−Ni ferromagnetic couplings increasing the shift of the lithium resonances.[30] Indeed, if only one near-neighbor nickel is required to couple a given nickel atom, the probability for a nickel ion not to be coupled is simply equal to $P(y,0)$. Hence, with this assumption, we get

$$I(y,1) = P(y,0)P(y,1) = P(y,0,1) \quad (6)$$

The experimental data would then show that more than one Ni−O−Ni coupling is required to induce a significant ferromagnetic interaction. Note that these couplings may also explain the low values of $I(y,0,2)$ and, especially, $I(y,0,3)$ for $y \leq 0.7$ (Figure 7c,d). They may likewise cause the increase in the line widths of the individual isotropic peaks with the number of nickel neighbors (Figures 4 and 5) and even give rise to the peak at ≈150 ppm (Figure 4a). In summary, all these observations are consistent with the fact that the ferromagnetic interactions increase with the local nickel concentration.

The Ni/Co segregation detected by NMR is indeed a small-scale phenomenon since it is not detected by X-ray diffraction (including Rietveld refinements). Furthermore, its magnitude is dependent on the preparation conditions and thermal history of the materials, as shown by Figure 9 in the case of two $y = 0.5$ samples (a and b). In addition to the initial heating and annealing at 900 °C (common to samples a and b), sample b has undergone a second thermal treatment at 900 °C with a subsequent quenching. This treatment decreased the intensity of component II from *ca.* 4% to 1%. Note that the latter value is close to what is expected in the case of a statistical Ni/Co distribution, since $P(0.5,0) = 1.56\%$ (Figure 7). By X-ray diffraction, the only observed effect of this thermal treatment is a slight narrowing of the peaks which could be, at least in part, attributed to the growth of the crystallites upon annealing.

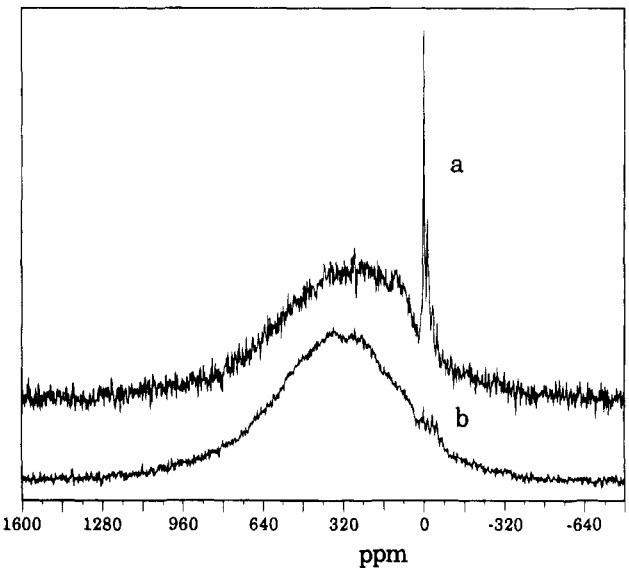

Figure 9. Effect of thermal history on the ^{6}Li MAS NMR spectrum ($B_0 = 7.1$ T) for $y = 0.5$: (a) sample prepared as described in the Experimental Section (same spectrum as in Figure 4a); (b) same sample that underwent a second annealing treatment at 900 °C.

Conclusion

^{6}Li and ^{7}Li high-speed MAS NMR is a valuable tool for studying the small-scale structure of the $LiNi_{1-y}Co_yO_2$ solid solution. Because the isotropic shift is very sensitive to the local environment of the lithium atoms, MAS NMR allows the precise determination of heterogeneities at the length scale of the chemical bond. Such slight deviations from a homogeneous Ni/Co distribution are invisible to X-ray diffraction since this technique requires long range order to be present.

Further NMR experiments will be performed in order to study in more details the dependence of this segregation on the preparation conditions and, more specifically, to see whether the Jahn−Teller character of the Ni^{3+} ion is the driving force for the segregation. Indeed, these microheterogeneities probably have a significant influence on the physical and electrochemical properties.

Acknowledgment. We are indebted to Dr. B. Meurer of the Institut Charles Sadron, Strasbourg, France, for permitting the use of the Bruker ASX-200 spectrometer. It is also a pleasure to acknowledge Dr. J. J. André and Dr. P. Panissod for helpful discussions. The UMR 50 CNRS-Bruker-ULP thanks the Région Alsace for its participation in the purchase of the Bruker MSL-300 spectrometer. C.M. thanks the CNRS and the Région Alsace for a stipend. M.M., A.R., and C.D. are grateful to the CNES for financial support.

IC940607E

(36) Anderson, P. W. *Phys. Rev.* **1959**, *115*, 2.